Ion chamber response and A_{wall} correction factors in a ^{60}Co beam by Monte Carlo simulation

D W O Rogers, A F Bielajew and A E Nahum†

Physics Division, National Research Council of Canada, Ottawa, Canada K1A 0R6

Abstract. The responses and wall correction factors for ion chambers in broad parallel ^{60}Co beams have been calculated using Monte Carlo techniques. The calculated responses are in good agreement with Bragg-Gray cavity theory. In particular, the response divided by the wall correction factor A_{wall} is found to be independent of the detector's shape but dependent on the material used for the chamber wall in a manner predicted by Bragg-Gray cavity theory. A simple theory is given which predicts the increase in response of a Farmer ion chamber due to an electrode of an arbitrary material and radius. The change in chamber response as a function of build-up cap composition is in good agreement with analytic expressions. The effect of guard regions in pancake chambers is found to be negligible. Embedding a pancake chamber in a flat phantom during calibration is shown to increase the response by $1.0 \pm 0.2\%$. Calculated values of A_{wall} are in good agreement with most experimental results and with those given in the AAPM protocol but with a considerably lower uncertainty of $\pm 0.2\%$. When using these values with the AAPM protocol, the β_{cep} factor should not be used since it is included in these calculated values.

1. Introduction

Both the AAPM protocol (1983) and NACP protocol (1980) for high energy radiation therapy dosimetry require knowledge of chamber dependent wall correction factors for ^{60}Co beams in order to convert an ion chamber's exposure calibration factor into its cavity-gas calibration factor N_{gas} (AAPM terminology) or its absorbed dose ionisation chamber factor N_D (NACP terminology). Any error or uncertainty in these ^{60}Co wall correction factors shows up directly in the final absorbed dose determination in a clinic. The NACP protocol presents a single value for this factor, based on the combined theoretical estimates and measurements of Johansson *et al* (1978), while the AAPM presents a set of correction factors for different chambers based on the Monte Carlo calculations of Nath and Schulz (1981) which have a stated statistical uncertainty of $\pm 0.4\%$ to 1.8%. The validity of the calculations by Nath and Schulz have been questioned because their calculated ion chamber responses do not agree with the predictions of cavity theory, the basis of all dosimetry protocols (Henry 1980, Nahum and Kristensen 1982). We have therefore used Monte Carlo techniques to calculate the wall correction factors and responses of ion chambers in broad parallel ^{60}Co beams. This paper is a more detailed presentation of an earlier report (Rogers *et al* 1983).

In an associated paper (Bielajew *et al* 1985) we have described the program CAVITY which simulates an ion chamber response to ^{60}Co. There it is shown that when the

† Permanent address: Department of Radiation Physics, University of Umeå, Sweden.

EGS Monte Carlo system is used for simulating radiation transport the results are very sensitive to the details of the electron transport algorithm. These details must be well understood, otherwise artefacts, which have no physical basis, alter the results.

In this paper we use the code CAVITY, first to confirm that ion chamber responses are calculated in accordance with cavity theory and then to investigate several problems of practical interest in radiation dosimetry, i.e. the effects on ion chamber response of (i) electrodes, (ii) varying the thickness of the wall relative to that of the build-up cap material, (iii) using a guarded region and (iv) using a phantom in the calibration procedure. We finish by presenting calculated wall correction factors for a wide variety of ion chambers and by comparing them to the values of Nath and Schulz and to measured values.

2. Theory

2.1. Terminology and Bragg–Gray cavity theory

We define chamber response R as the absorbed dose to the cavity gas divided by $K_{\text{col,air}}$, the collision kerma in air at the geometric centre of the ion chamber in the absence of the chamber. The exposure at the centre of the ion chamber in its absence is given by, $X = K_{\text{col,air}} e / W$ (Attix 1979). Under the assumptions that (i) the photon beam is not attenuated or scattered in the chamber walls, (ii) the chamber cavity does not perturb the electron fluence and (iii) charged particle equilibrium is established at the chamber cavity, then Bragg-Gray cavity theory gives the normalised chamber response to be

$$R^{\text{CAV}} = s_{\text{air,wall}}(\mu_{\text{en}}/\rho)_{\text{air}}^{\text{wall}} \tag{1}$$

where $s_{\text{air,wall}}$ is the stopping power ratio (see for example Spencer and Attix 1955, ICRU 1984) and $(\mu_{\text{en}}/\rho)_{\text{air}}^{\text{wall}}$ is the ratio of mass energy absorption coefficients in the wall to those in air averaged over the primary photon spectrum. For air equivalent walls $R^{\text{CAV}} \equiv 1.00$ (R^{CAV} is equivalent to k_{m} in the NACP protocol).

If we remove the assumption of no attenuation or scatter in the chamber walls, then

$$R = R^{\text{CAV}} A_{\text{wall}} \tag{2}$$

where R is the normalised chamber response including the effects of attenuation and scatter and R^{CAV} is the normalised chamber response ignoring these effects. The wall correction factor A_{wall} takes into account a decrease in the response because of attenuation of the primary photons in the walls and an increase because of photons scattered in the walls. Unlike the formalism in the AAPM protocol, A_{wall} as we use and calculate it includes the effects of electron transport and therefore includes the β_{cep} correction factor (see § 3.7 below).

There are two common approaches to calculating the factor R^{CAV}. One, the basic Bragg-Gray approach, evaluates the stopping power using the primary electron spectrum and unrestricted collision stopping power to calculate $s_{\text{air,wall}}^{\text{BG}}$ and hence R^{BG}. The underlying assumption is that knock-on electrons deposit their energy locally. This requires charged particle equilibrium (including knock-on electrons) in the cavity. Under this assumption $R^{\text{CAV}} = R^{\text{BG}}$ is completely independent of the geometry of the cavity.

The second common approach is the Spencer-Attix formulation of Bragg-Gray cavity theory in which knock-on electrons above some cutoff Δ are explicitly included

in the electron spectrum when evaluating $s_{\text{air,wall}}^{\text{SA}}$ using restricted stopping powers L_Δ/ρ. In this case R^{SA} might be dependent on the geometry of the cavity through the dependence of s^{SA} on the cavity dimensions in a way determined by the value of Δ. However, as can be seen from table 1, the dependence of R^{SA} on Δ and hence on the geometry is very small for carbon and only somewhat larger for aluminium. The values of $s_{\text{air,wall}}$ used to calculate the values in table 1 were based on electron spectra, both total and primary, calculated at the peak of the depth–dose curve in roughly 1 g cm^{-2} thick phantoms for broad parallel beams of ^{60}Co. The calculations of s^{SA} took explicit account of energy deposition by track ends (Nahum 1978).

Table 1. Evaluation of R^{CAV} using the basic Bragg–Gray approach to calculate $s_{\text{air,wall}}^{\text{BG}}$ and the Spencer–Attix approach to calculate $s_{\text{air,wall}}^{\text{SA}}$ as a function of Δ. The Berger and Seltzer (1964) stopping powers were used. $R^{\text{CAV}} = s_{\text{air,wall}}(\mu_{\text{en}}/\rho)_{\text{air}}^{\text{wall}}$.

Material	$(\mu_{\text{en}}/\rho)_{\text{air}}^{\text{wall}}$	R^{BG}	R^{SA}			
			$\Delta = 10$ keV	$\Delta = 15$ keV	$\Delta = 20$ keV	$\Delta = 50$ keV
Carbon	1.0015†	0.995	0.993	0.993	0.994	0.995
Aluminium	0.962‡	1.087	1.105	1.101	1.098	1.091

† Based on Hubbell (1977).
‡ Based on an energy interpolation of Hubbell (1969).

When calculating the responses of very large chambers, we were concerned that assumption (ii) might break down. However, as long as air-equivalent walls are used, Fano's theorem (see for example Burlin 1968) implies that $R/A_{\text{wall}} = 1.00$. This condition provided a useful constraint for checking our code under extreme geometric conditions.

2.2. Method of calculation

The computer code CAVITY which is used to calculate ion chamber response in a ^{60}Co beam can, in addition, both keep track of the wall from which the electrons entered the cavity and calculate A_{sc} and A_{at}, the correction factors for scattering and attenuation in the walls (Bielajew *et al* 1985). These were calculated as follows. Let

$$R_{\text{tot}} = \sum_i (r_i^0 + r_i^1)$$

where R_{tot} is the total energy deposited in the cavity gas, r_i^0 is the energy deposited by the electrons generated by the ith primary photon interaction and r_i^1 is the energy deposited by electrons generated from the second or higher order scattered photons that arise from the ith primary photon. Then

$$A_{\text{sc}} = R_{\text{tot}} \bigg/ \sum_i r_i^0 \geqslant 1$$

$$A_{\text{at}} = R_{\text{tot}} \bigg/ \sum_i (r_i^0 + r_i^1)\, \mathrm{e}^{+d_i} \leqslant 1$$

$$A_{\text{wall}} = A_{\text{sc}} A_{\text{at}}$$

where d_i is the number of primary photon mean free paths to the point of interaction of the ith primary photon in the chamber. A_{sc} represents the fractional increase in the response due to scattered photons (and hence is $\geqslant 1$). A_{at} represents the fractional

decrease in the response due to attenuation of the ^{60}Co beam in the chamber. The e^{+d_i} term increases the response to correct for primary photon attenuation in the chamber. Note that d_i accounts for passage through the chamber walls, end caps, electrode, build-up cap and cavity-gas.

The efficiency of the A_{sc} calculation is enhanced by forcing all scattered photons to interact a second time in the chamber (see the discussion of variance reduction in Bielajew *et al* 1985). Since these factors are obtained from ratios of correlated numbers, they have a much smaller statistical uncertainty than the calculated total response and are much less sensitive to parameter selection.

The following parameters, as discussed in Bielajew *et al* (1985), have been used for all calculations unless otherwise stated: maximum fractional energy loss per step, ESTEPE = 0.01; step size, SMAX = 0.2 cm; transport control parameters, ECUT = PCUT = AE = PCUT = AP = 10 keV. The calculations were done for broad parallel beams. The same results would be expected for point sources at normally used SSDs. To obtain statistical uncertainties of the order of 1% required 5-24 h of CPU time on a Vax 11/780 with floating point acceleration.

3. Results

### 3.1. Pancake chamber response as a function of radius and depth

Nath and Schulz (1981) calculated the response to ^{60}Co of a 3.3 mm deep pancake chamber with 0.55 g cm^{-2} carbon walls as a function of the radius of the chamber. Contrary to expectations of Bragg-Gray cavity theory as discussed in § 2.1, they found a 10% variation in R/A_{wall} as the radius changed from 0.1 to 10 cm. Our calculations for a similar chamber (2 mm deep with 0.5 g cm^{-2} walls) are presented in figure 1(a). The results show no variation as a function of radius, as well as being in good agreement with the absolute predictions of Bragg-Gray theory.

Our results are normalised by $K_{col,air}$, the air collision kerma at the geometric centre of the chamber. The conversion factor from fluence to $K_{col,air}$ was calculated using EGS by scoring the total air kerma per unit fluence incident on an air slab and correcting for 0.4% bremsstrahlung losses (NACP 1980). The resulting value of 5.333×10^{-12} Gy cm^2 is only 0.04% lower than the value determined using Hubbell's μ_{en}/ρ value for carbon of 2.662×10^{-3} m^2 kg^{-1} (Hubbell 1977).

Figure 1(b) presents R/A_{wall} as a function of the internal depth of the cavity for a pancake chamber with a radius of 1 cm. Our results show no deviation from the virtually constant R^{SA} predicted by equation (1) although the results of Nath and Schulz show a slight variation. For chambers which are much deeper than those used in practice, our results for A_{wall} are significantly lower than those of Nath and Schulz. These differences are due to the fact that our calculations are for a parallel beam and those of Nath and Schulz are for a point source at 100 cm. Our results for a point source are in good agreement with those of Nath and Schulz.

3.2. Response as a function of wall material

As well as predicting only a very small dependence of R/A_{wall} on the geometry of the chamber for the low Z materials we are studying, Bragg-Gray cavity theory makes a direct prediction of the absolute response of the chamber for different wall materials in terms of R^{CAV} as given by equation (1). Table 2 compares our Monte Carlo calculated
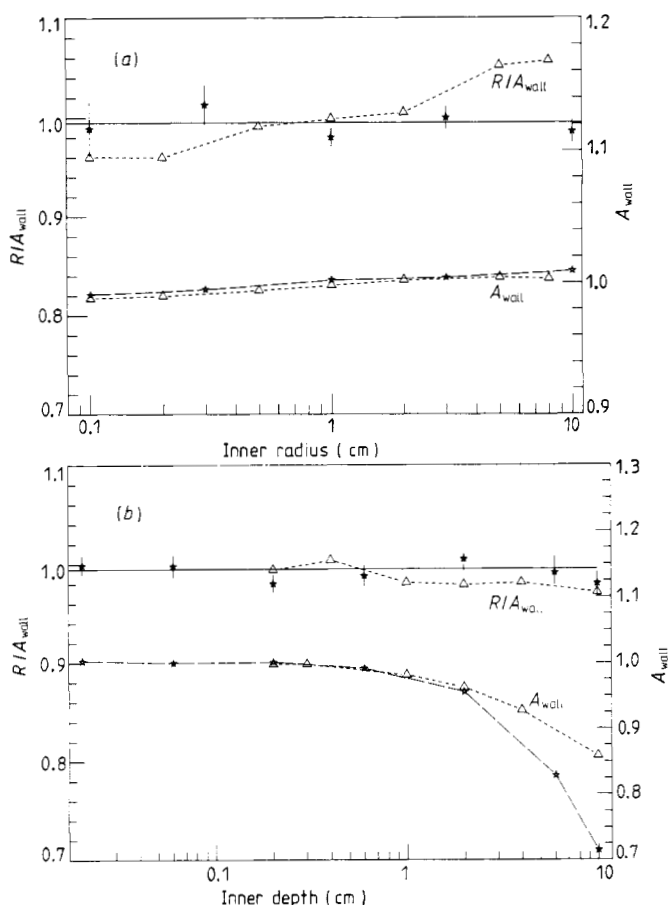
Figure 1. Calculated R/A_{wall} and A_{wall} values for a carbon walled pancake ion chamber irradiated by a ^{60}Co beam (a) as a function of chamber inner radius with a cavity depth of 2 mm and 3 mm for ★, the present results and △, the Nath and Schulz results respectively and (b) as a function of chamber inner depth with an inner radius of 1 cm. The present results are for parallel beam incident on a 0.5 g cm^{-2} walled chamber, whereas the Nath and Schulz results are for a point source 100 cm from a 0.55 g cm^{-2} walled chamber. ——, R/A_{wall} predicted by basic Bragg–Gray cavity theory. In all our calculations, carbon is assumed to have a density of 1.83 g cm^{-3}. The differences in A_{wall} at large depths shown in (b) are due solely to the difference between the point source and parallel beam calculation.

values of R/A_{wall} with the Bragg–Gray values of R^{CAV} predicted using either the basic Bragg–Gray or Spencer–Attix prescriptions for $s_{gas,wall}$. There is reasonable agreement within the statistical uncertainties of the Monte Carlo results. With the exception of the aluminium walled chamber, the results of Nath and Schulz (for spherical chambers with a radius of 1 cm) are consistent with our values. This is fortuitous in view of the discrepancies reported in the previous section, but consistent with those results where the Nath and Schulz results 'crossed ours' for radii ≈ 1 cm.

Experimental results for the ratio of R^{CAV} for an aluminium chamber to that for a carbon chamber of 1.07 ± 0.01 (Nahum and Kristensen 1982) and 1.102 ± 0.005 (Nahum *et al* 1985) are consistent with our calculated result of 1.085 ± 0.013.

Our Monte Carlo calculations were based on the 1964 stopping powers and should be compared to R^{CAV} evaluated using these values. The predictions based on the latest

Table 2. Comparison of Bragg-Gray predicted values of R^{CAV} (equation 1) as a function of wall material and the comparable Monte Carlo calculated values of R/A_{wall}. The R^{CAV} values are calculated using Bragg-Gray cavity theory considering the primaries only (R^{BG}) or using the Spencer-Attix formulation (R^{SA}) which takes into account knock-on electrons. A set of values computed using the 1983 electron stopping powers is given in order to indicate the size of changes these imply but the current Monte Carlo calculations were done with 1964 electron stopping powers. $R^{CAV} = s_{air,wall}(\mu_{en}/\rho)_{gas}^{wall}$.

Material		R/A_{wall} (Monte Carlo)	$R^{BG f}$	$R^{SA f}$ ($\Delta = 10\,keV$)	$R^{SA g}$ ($\Delta = 10\,keV$)	R/A_{wall} Nath and Schulz (1981)[h]
Aluminium		$1.059 \pm 0.7\%$[a]	1.087	1.105	1.116[j]	1.014
		$1.089 \pm 0.6\%$[b]				
	Av.	$1.074 \pm 0.5\%$				
Carbon		$0.983 \pm 0.6\%$[c]	0.995	0.993	1.001[i]	0.985
		$0.993 \pm 1.0\%$[b]				
	Av.	$0.988 \pm 0.6\%$				
PMMA[e]		$0.958 \pm 0.5\%$[a]	0.973	0.967	0.982	0.963
Polystyrene[e]		$0.963 \pm 0.6\%$[d]	0.966	0.959	0.972	0.961

[a] Thimble chambers, 0.315 cm inner radius, 2.5 cm inner length, no electrode, 0.5 g cm^{-2} walls (and 0.74 g cm^{-2} in the case of Al).
[b] Pancake chambers discussed in § 3.1 averaged over various dimensions, 0.5 g cm^{-2} walls. The difference between aluminium thimble and pancake chambers is most likely due to statistical fluctuations.
[c] Average for thimble chambers with carbon electrodes of various radii (§ 3.3), 0.315 cm inner radius, 2.5 cm inner length, 0.5 g cm^{-2} walls.
[d] For pancake chamber defined in § 3.5 averaged over various phantom sizes.
[e] R^{CAV} values calculated using electron spectrum calculated in carbon.
[f] Berger and Seltzer (1964).
[g] Berger and Seltzer (1983).
[h] Taken from Nahum and Kristensen (1982, table 1).
[i] Using a density effect correction based on $\rho_{carbon} = 1.7$ g cm^{-3}.
[j] Using the standard density effect correction.

electron stopping powers (Berger and Seltzer 1983) are included to indicate where changes are expected.

3.3. Response as a function of electrode radius and material

For the low Z materials we are interested in, Bragg-Gray cavity theory predicts no significant dependence of R/A_{wall} on cavity geometry and hence there should be no dependence on electrode radius as long as it is made of the same material as the walls. Our results in figure 2 show no significant variation in R/A_{wall} ($\leqslant 1.7\%$ spread) or A_{wall} ($\leqslant 0.3\%$ spread) as a function of electrode radius for a carbon electrode in a carbon walled chamber. This is in contrast to the 7% variation in response reported by Nath and Schulz. We have also simulated the cylindrical graphite chamber ($r = 0.8$ cm, 0.55 g m^{-2} carbon walls, assumed 4 cm long) for which McEwan and Smyth (1984) have calculated A_{wall} as a function of electrode radius. Our results show the same trend as theirs but are somewhat lower.

On the other hand, when the electrode is made of a different material than the walls, some variation in response is expected, in the same way that chamber response is dependent on wall material as shown in the previous section. Figure 2 presents our calculated results for an aluminium electrode in a carbon walled Farmer chamber.
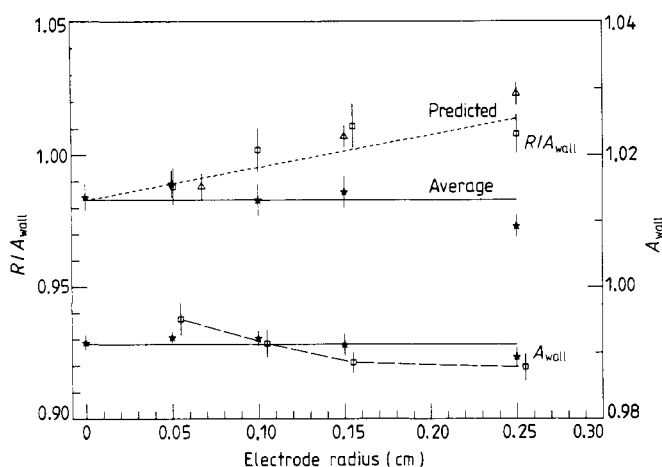
Figure 2. R/A_{wall} and A_{wall} for a carbon walled Farmer ion chamber as a function of electrode material and radius. $\star$, carbon electrode; $\square$, aluminium electrode. The chamber had 0.5 g cm^{-2} walls, an internal radius of 0.315 cm and a cavity length of 2.5 cm. The line marked 'average' is the average value of R/A_{wall} for the carbon electrode cases. $\triangle$, the experimental values of Kristensen for an aluminium electrode, normalised to our results without an electrode and divided by our calculated values of A_{wall}. The line marked 'predicted' gives the values predicted by the simple model described in § 3.3.

There is an increase in the R/A_{wall} of up to 2.7% with the aluminium electrode. There may also be a slight variation in A_{wall}, but the statistical uncertainties are large compared with this possible effect. Figure 2 shows our results compared with the experimental results of Kristensen (1983) for R/A_{wall}, after normalising to our calculated response with no electrode and using our computed values of A_{wall}. There is good agreement.

These results for the increased response with an aluminium electrode are exactly those expected from a simple extension of Bragg–Gray cavity theory. With the help of a simple model, the change in response can be calculated for electrodes made of any material. The model assumes that the fraction of the chamber's response from electrons coming from the electrode is increased by the ratio R^{CAV} (electrode)$/R^{\mathrm{CAV}}$ (wall). Then

$$R_{\mathrm{el}}(F_{\mathrm{el}})/A_{\mathrm{wall}} = (1 - F_{\mathrm{el}})R^{\mathrm{CAV}}(\mathrm{carbon}) + F_{\mathrm{el}}R^{\mathrm{CAV}}(\mathrm{electrode}) \qquad (3)$$

where $R_{\mathrm{el}}(F_{\mathrm{el}})$ is the response of the chamber with a different electrode material and F_{el} is the fraction of the dose to the air in the cavity delivered by electrons entering the cavity from a carbon electrode of the same radius.

Table 3 presents our Monte Carlo calculated values of F_{el} for a carbon walled Farmer chamber and the increase in response for an aluminium electrode as predicted by this simple model. The predicted change is shown in figure 2 as a broken line. It agrees well with the calculated and measured values.

3.4. Response for composite wall

Although the results presented to this point are for chambers with walls of a single material, it is common practice for chambers to have walls of one material and a build-up cap of another. In figure 3 we present the calculated change in response for a 0.5 g cm^{-2} walled chamber as we make the transition from a PMMA chamber to a carbon walled chambeı with a PMMA build-up cap and finally to a pure carbon walled

Table 3. The increase in R/A_{wall} as a function of the radius of an aluminium electrode as predicted by equation (3) and the fraction of dose to the air in the cavity delivered by electrons entering from a central carbon electrode in a 0.5 g cm^{-2} carbon walled Farmer chamber with an inner length of 2.5 cm and inner radius of 0.315 cm.

Electrode radius (cm)	Increase with an aluminium electrode (%)†	F_{el}
0.0	0.0	0.00
0.05	+0.8	0.092
0.10	+1.5	0.17
0.15	+2.0	0.23
0.25	+3.1	0.36

† Using Monte Carlo value of $R^{CAV}(Al)/R^{CAV}(C) = 1.087$ from table 2, second column.

chamber. There is no change in the calculated values of A_{wall} to within 0.1% while the response increases by the 2.5% expected based on the results of table 2.

The AAPM protocol (1983, equation 6) gives an expression for the response of a carbon chamber with build-up cap. This can be rewritten as

$$R/A_{wall} = \left(\frac{\alpha}{R^{CAV}(wall)} + \frac{(1-\alpha)}{R^{CAV}(cap)} \right)^{-1} \qquad (4)$$

where α is the fraction of the ionisation due to electrons from the chamber wall and $(1-\alpha)$ is the fraction of ionisation from electrons from the build-up cap. Using the values of α given in the AAPM protocol and our Monte Carlo calculated values of R^{CAV} for Farmer chambers of carbon and PMMA (table 2) gives the broken curve in figure 3. It is in excellent agreement with our calculated results.
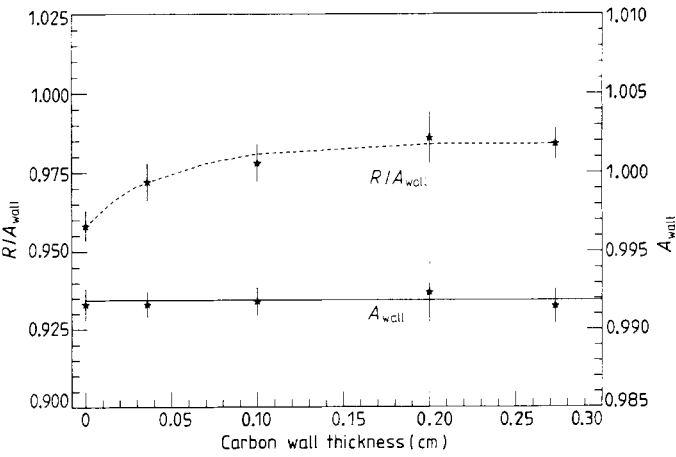
Figure 3. R/A_{wall} and A_{wall} for a 2.5 cm long Farmer ion chamber with walls plus build-up cap totalling 0.5 g cm^{-2} thickness for different combinations of carbon wall and PMMA build-up cap, going from a pure PMMA to a pure carbon walled chamber. ★, present results. - - - -, values predicted by equation (4) (developed from the AAPM protocol).

3.5. Response of guarded chambers

Pancake chambers, such as the Memorial Sloan-Kettering (MSK) chamber, have a guarded sensitive volume, i.e. only the ionisation from the central region of the cavity is collected. The question arises as to whether A_{wall} and R for the guarded region are the same as for the entire cavity. To investigate possible variations we have carried out calculations for the MSK chamber (cavity radius 17.5 mm, depth 2 mm, front and back walls 4 mm thick, edge walls 5 mm thick, made of polystyrene, radius of sensitive volume 12.7 mm). The sensitive volume makes up about 50% of the cavity. The values for A_{wall} and R/A_{wall} given in table 4 indicate no significant differences between the guarded region and the entire cavity.

Table 4. Values of A_{wall} and R/A_{wall} for the guarded sensitive volume (radius 12.7 mm) and entire cavity region (radius 17.5 mm) for the Memorial Sloan-Kettering pancake chamber.

	A_{wall}	R/A_{wall}
Guarded region	$1.0032 \pm 0.06\%$	$0.953 \pm 0.8\%$
Entire cavity	$1.0025 \pm 0.04\%$	$0.956 \pm 0.6\%$

3.6. Effect of a phantom on chamber response and A_{wall}

In general, A_{wall} correction factors are used for ^{60}Co calibrations of ion chambers when no phantoms are involved. However, some chambers, e.g. the MSK pancake chamber, come embedded in one slab of a polystyrene phantom which is present during ^{60}Co calibrations. We have investigated the effect of this phantom by treating it as part of the chamber and calculating the response and A_{wall} as the outer radius of the chamber is increased. Figure 4 shows that, as expected, R/A_{wall} is independent of the radius of phantom the chamber is embedded in. On the other hand the value of A_{wall} increases by 1% from the value for the 'bare' chamber of $1.0025 \pm 0.05\%$ to a value of $1.013 \pm 0.2\%$ for an effectively infinite phantom (i.e. phantom diameters $\geqslant 10$ cm). The increase
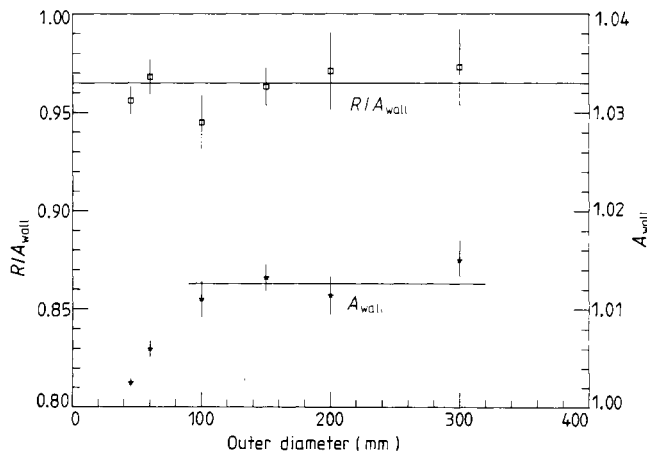


Figure 4. Calculated values of ★, A_{wall} and □, R/A_{wall} for the MKS pancake ion chamber as the thickness of the curved wall is increased to simulate the polystyrene phantom in which the chamber is embedded for ^{60}Co calibrations. ——, R/A_{wall} predicted by basic Bragg-Gray cavity theory.

comes entirely from the scatter component of the response which increases from 2.1% for the bare chamber to 3.1% for the chamber embedded in a phantom with a diameter greater than 10 cm. These values are to be compared to the A_{wall} value of 1.008 given in the AAPM protocol for the MSK chamber but which appears to apply to a chamber with uniform 4.7 mm thick walls.

3.7. Calculated values of A_{wall}

Unlike the chamber response, which has been shown to depend strongly on the fractional energy loss per electron step (Bielajew *et al* 1985), the calculated values of A_{wall} are virtually independent of the electron step size used. This is shown in figure 5 where A_{wall} is shown to be constant within the statistical uncertainty of the calculation
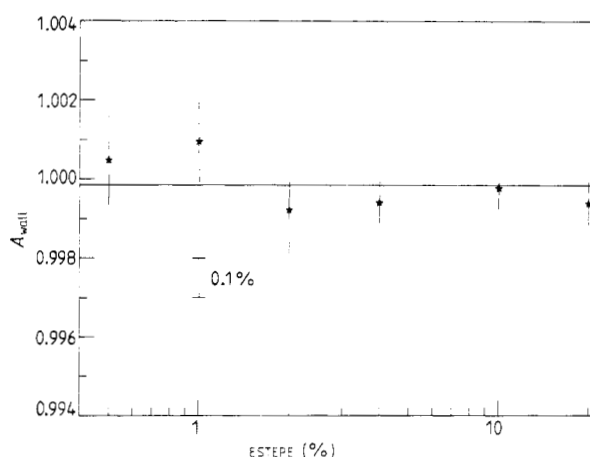
Figure 5. Variation in A_{wall} for a carbon walled pancake chamber as the maximum fractional energy loss per electron step ESTEPE is varied. ——, average value.

($\leqslant 0.1\%$). This should be compared to the 70% change in calculated response for the same values of ESTEPE. To speed up the calculations by nearly a factor of four, we have carried out A_{wall} calculations with ESTEPE = 4% instead of 1% as used for the response calculations.

In table 5 we present our results for various ionisation chambers and compare them to those of Nath and Schulz (mostly using the specification of the chambers given by Nath and Schulz). Based on the results of § 3.4 (figure 3), the value of A_{wall} does not depend on the distinction between wall and build-up cap material, so the calculations were done for the uniform walls specified in table 4. Since the electrode has been shown in § 3.3 to have at most a small effect on A_{wall}, we have treated the electrodes in cylindrical chambers as extending the full length of the chamber in most cases. The MSK pancake chamber appears to have been incorrectly specified in the AAPM protocol, using the sensitive radius instead of the cavity radius. Based on figure 1(*a*), our value would be only 0.07% smaller for the bare chamber with the smaller radius. Thus this difference does not explain the difference in our calculated values of A_{wall} for the MSK chamber and that given in the AAPM protocol.

Nath and Schulz (1981) quote statistical uncertainties of ±0.3–0.7% on their values of A_{wall}. However, the data in their table IV suggests a statistical uncertainty of $\leqslant 0.1\%$

Table 5. Calculated A_{wall} correction values for specific ionisation chambers. Estimates of one standard deviation uncertainties in the last digit are shown in brackets. Shapes of chamber are: C, cylindrical; CS, cylindrical shell; P, pancake; and DP, double pancake.

Chamber	Shape	Cavity dimensions Radius (cm)	Cavity dimensions Length (cm)	Electrode Material	Electrode Radius (cm)	Electrode Length (cm)	Wall + build-up Material	Wall + build-up Total thickness (g cm^{-2})	$(A_{sc}-1)\times100$	$(1-A_{at})\times100$	A_{wall} Present results	A_{wall} Nath and Schulz	A_{wall} Δ(%)
Capintec-Farmer, 0.6 cm^3	C	0.325	2.380	Al	0.080	2.380ᵃ	PMMA	0.668	3.11 (7)	4.21 (7)	0.9877 (7)	0.9900 (40)	+0.23
Capintec, 0.1 cm^3	C	0.200	0.550	Al	0.050	0.550ᵃ	C	0.550	2.38 (1)	3.24 (1)	0.9907 (7)	0.9910 (50)	+0.03
Capintec, pancake	P	0.800	0.240	—	—	—	Polyᵈ	0.573	2.59 (4)	2.92 (1)	0.9959 (4)	0.9950 (90)	-0.09
PTW normal	C	0.250	1.800	Al	0.050	1.800ᵃ	PMMA	0.420	1.95 (6)	2.48 (1)	0.9942 (6)	0.9940 (40)	-0.02
PTW transit	C	0.450	2.300	Al	0.075	2.300ᵃ	PMMA	0.450	2.26 (4)	3.04 (1)	0.9914 (5)	0.9940 (30)	+0.26
PTW micro	C	0.350	1.200	Al	0.050	1.200ᵃ	PMMA	0.570	2.69 (8)	3.68 (1)	0.9891 (8)	0.9880 (50)	-0.11
Shonka 0.1 cm^3	C	0.225	1.150	Al	0.075	1.150ᵃ	PMMA	0.605	2.66 (7)	3.67 (1)	0.9889 (7)	0.9890 (70)	+0.01
EXRADIN A.E.	CS	0.450	0.854	C	0.230	0.854ᵇ	C	1.072	5.18 (6)	7.27 (1)	0.9753 (6)	0.9730 (80)	-0.24
BIPM	DP	2.250	2×0.205	C	2.250ᵃ	0.100	C	0.522ᵃ	2.94 (9)	2.92 (1)	0.9993 (10)	0.9970 (40)	-0.24
NBS	CS	0.475	1.060	C	0.350	1.060ᶜ	C	0.481	3.14 (7)	4.47 (2)	0.9853 (7)	0.9830 (40)	-0.23
MSKCC	C	0.250	0.500	Polyᵈ	0.050	0.500ᵃ	Polyᵈ	0.524	2.20 (7)	3.16 (1)	0.9897 (7)	0.9900 (180)	+0.03
MSKCC	C	0.500	0.500	Polyᵈ	0.050	0.500ᵃ	Polyᵈ	0.524	2.60 (7)	4.21 (1)	0.9862 (7)	0.9850 (160)	-0.12
NRCC standard	CS	0.792	1.614	C	0.335	1.200	C	0.701ᵉ	—	—	0.9764 (12)	—	—
MSK	P	1.750ᶠ	0.200	—	—	—	Polyᵈ	0.424ᵍ	{ 2.04 (8) / 3.0 (2) }	{ 1.85 (1) / 1.86 (3) }	{ 1.0025 (5)ʰ / 1.0130 (20)ⁱ }	1.0080	+0.55
Nuclear Enterprises Farmer	C	0.314	2.500	Al	0.050	2.500	PMMA	0.613	2.86 (7)	3.77 (1)	0.9899 (7)	—	—
PTB 0.5 cm^3	C	0.300	2.000	—	—	—	C	0.520ʲ	2.28 (7)	3.11 (2)	0.9909 (17)	—	—
PTB 1.5 cm^3	C	0.500	2.000	—	—	—	C	0.520ʲ	2.64 (9)	3.69 (3)	0.9885 (9)	—	—
PTB	DP	2.200	2×0.200	C	2.200	0.050	C	0.690	3.64 (9)	3.60 (1)	0.9993 (7)	—	—

ᵃ Differs from Nath and Schulz (1981) in most cases by simulating a full length electrode.
ᵇ Actually 0.62 cm; in the limit of no electrode, $A_{wall} = 0.9756$ (8).
ᶜ Electrode actually 0.80 cm; in the limit of no electrode, $A_{wall} = 0.9862$ (7), $\Delta = 0.09 \pm 0.10\%$.
ᵈ Poly = polystyrene.
ᵉ This is the cylindrical wall; end caps 0.835 g cm^{-2}.
ᶠ This is the cylindrical wall; in AAPM protocol which gives the radius of the guarded region only (see § 3.5).
ᵍ Differs from value in AAPM protocol; differs from AAPM which gives 0.500 g cm^{-2}.
ʰ Thickness of front and back wall only; (i.e. bare wall). Figure 1 suggests a value of 1.0018 if $r = 1.27$ cm as in AAPM protocol.
ⁱ Value for 0.530 g cm^{-2} side walls (i.e. bare chamber). Figure 1 suggests a value of 1.0018 if $r = 1.27$ cm as in AAPM protocol.
ʲ Value for infinite side walls as in the phantom.
ᵏ PTB cylindrical chambers had end caps 0.607 g cm^{-2}.

since there is a very small spread in their results for the 'full simulations' versus those based on the 'interpolations' from their table III. This is further confirmed by the average difference of $0.04 \pm 0.17\%$ between their results and ours (excluding the MSK pancake chamber which is only given in the AAPM protocol). Based on table 5, $\pm 0.2\%$ appears to be a conservative estimate of the uncertainty of our calculated values of A_{wall}.

As mentioned in § 2.1, our calculated values of A_{wall} include the effects of electron transport and therefore include the β_{cep} factor, i.e. $A_{\text{wall}}^{\text{Monte Carlo}} = A_{\text{wall}}^{\text{AAPM}} \beta_{\text{cep}}$. This is contrary to the interpretation given in the AAPM protocol but in agreement with the interpretation of Nath and Schulz (1981), Attix (1984) and Schulz and Loevinger (1984). Our $A_{\text{wall}}^{\text{Monte Carlo}}$ value is k_{att} in the NACP protocol.

3.8. Comparison of A_{wall} values with experiment

In table 6 we have compared our calculated values of A_{wall} with a variety of measured values. Our calculated values should be compared to the measured A_{wall} values including β_{cep}. In all cases the 'measured' values include a theoretical correction factor for β_{cep}. We have given the values with and without this calculated value because of the uncertainty in this factor. For example, $\beta_{\text{cep}} = 1.0076$ or 1.0029 were used by the

Table 6. Comparison, with and without the β_{cep} correction factors, of experimental measurements of A_{wall} to the calculated values. Chamber dimensions are given in table 5 except for the spherical NBS chambers which had 0.688 g cm^{-2} (1 cm^3) and 0.647 g cm^{-2} (10 cm^3) thick carbon walls. The differences between calculation and measurement are shown in brackets below the measured values.

		A_{wall}	
	Calculated	Measured	
Chamber		Including β_{cep}	Excluding β_{cep}
BIPM double pancake chamber[a]	0.9993 (10)	0.9963 (23)	0.9888 (23)
	0.997 (4)[e]	(-0.3%)	(-1.0%)
NRC cylindrical shell[b]	0.9764 (12)	0.9786 (20)	0.9737 (20)
		$(+0.23\%)$	(-0.27%)
NBS 1 cm^3 [c]	0.981 (5)[e]	0.9884 (20)	0.9835
		$(+0.7\%)$	$(+0.2\%)$
NBS 10 cm^3 [c]	0.980 (6)[e]	0.984	0.979
		$(+0.4\%)$	(-0.1%)
Farmer[d]	0.9897 (7)	0.990	0.985
		$(+0.03\%)$	(-0.5%)
PTB 0.5 cm^3 [f]	0.9909 (7)	0.9909 (16)	0.9879 (5)
		(0.00%)	(-0.3%)
PTB 1.5 cm^3 [f]	0.9885 (9)	0.9904 (18)	0.9875 (9)
		$(+0.19\%)$	(-0.11%)
Double pancake	0.9993 (7)	0.9932 (25)	0.9903 (20)
		(-0.6%)	(-0.9%)

[a] Boutillon and Niatel (1973).
[b] Henry (1980).
[c] Loftus and Weaver (1974) and Niatel *et al* (1975).
[d] Johansson *et al* (1978).
[e] From table I of Nath and Schulz (1981). As discussed in § 3.7, we believe their statistical uncertainties are actually $\leq \pm 0.2\%$; however, we cannot check their A_{wall} calculations for spherical chambers although they appear to be in reasonable agreement with the values of McEwan and Smyth (1984).
[f] Niatel *et al* (1975).

BIPM and PTB for essentially the same chamber. For the cylindrical and pancake chambers agreement between the calculated and measured values is within the combined uncertainties for all chambers except the PTB pancake chamber. The values calculated by Nath and Schulz for the NBS spherical chambers are low compared to experiment but this difference is only statistically significant if it is accepted that their estimated statistical uncertainties for spherical chambers are too high, as we have demonstrated is the case for their cylindrical chambers.

3.9. Origin of electrons

In § 3.3 we made use of a facility in CAVITY which specifies by which surface an electron enters an ion chamber. In that case we found that, for example, 9% of the response in a Farmer chamber comes from electrons leaving the 0.05 cm radius carbon electrode. In the same chamber, 4.5% of the response comes from each end cap and 82% of the response comes from the wall. If we consider a pancake chamber such as the MSK chamber defined in § 3.5, the response is due to electrons from the front wall (70%), the side wall (9%) and the back wall (20%). In the aluminium pancake chamber discussed in § 3.1, the 1 cm radius chamber derived 26% of its response from electrons leaving the back wall. EGS calculates that about 13% of normally incident electrons in the 300–500 keV range are reflected from silicon which is similar to aluminium (Rogers 1984) and thus we would expect an even larger fraction of obliquely incident electrons to be reflected from the back wall of the ion chamber. Thus a large portion of our so-called response 'from the back wall' is from electrons generated in the front or side walls and reflected from the back wall.

A similar effect is noted if we calculate the change in the response of the BIPM's double pancake chamber (specified in table 5) as the side wall thickness is changed. As we go from the full side wall to a 0.05 g cm^{-2} and then to a zero thickness wall, the response decreases by $4.0 \pm 0.8\%$ and $14.2 \pm 1.1\%$ in good agreement with the measured and extrapolated values of 3.8% and 14% (Boutillon and Niatel 1973). However, for the complete chamber, only $7.4 \pm 0.5\%$ of the response is calculated to be due to electrons from the side wall. The 'other' 7% of the dose due to electrons originating in the side walls is scored as electrons reflected from the electrode or back wall.

4. Conclusions

Our results demonstrate that careful Monte Carlo simulations of ion chamber response in ^{60}Co beams are in good agreement with the predictions of Bragg–Gray cavity theory and the available experimental data. We have developed a simple model to predict the effect on a Farmer chamber's response of an electrode of arbitrary material and radius. Our results are in good agreement with current estimates of the effects of build-up caps. We find no effects due to the use of guard rings in pancake ion chambers but do find that the MSK chamber's response in a ^{60}Co beam is increased by about 1% because of the slab in which it is placed.

Despite a marked difference in calculated values of chamber response the results presented by Nath and Schulz for A_{wall} are generally in good agreement with ours. This is consistent with the fact that our A_{wall} values are much less sensitive to the details of the calculation than our calculated chamber responses. We found that ±0.2% represents a conservative estimate of the statistical uncertainty of our calculated values

of A_{wall}. If wall correction factors calculated with Monte Carlo techniques are used in the AAPM protocol, then the β_{cep} (called β_{wall} in the protocol) factor included there should not be used, i.e. the AAPM protocol, as presented, overestimates absorbed doses by 0.5% due to this extra inclusion of β_{cep}.

Résumé

Réponse de la chambre d'ionisation et facteurs de correction A_{paroi} dans un faisceau de cobalt, obtenus par la méthode de Monte Carlo.

Les réponses et les facteurs de correction de paroi pour des chambres d'ionisation ont été calculés par les techniques de Monte Carlo pour des faisceaux larges et parallèles de rayons γ du ^{60}Co. Les réponses calculées sont en bon accord avec la théorie de la cavité de Bragg-Gray. Il apparaît en particulier que la réponse, divisée par le facteur de correction A_{paroi}, est indépendante de la forme du détecteur, mais dépend du matériau utilisé pour la paroi de la chambre, conformément à ce que prévoit la théorie de la cavité de Bragg-Gray. L'augmentation de la réponse d'une chambre d'ionisation Farmer, avec une électrode de matériau et de rayon arbitraires, peut être prévue à l'aide d'une théorie simple. La variation de la réponse de la chambre en fonction de la composition du capuchon d'équilibre électronique est en bon accord avec les expressions analytiques. On trouve que l'effet de l'anneau de garde dans les chambres plates est négligeable. Les auteurs ont également montré que la réponse de la chambre plate, placée dans un fantôme, est augmentée de $1{,}0 \pm 0{,}2\%$. Les valeurs calculées pour A_{paroi} sont en bon accord avec la plupart des résultats expérimentaux et avec ceux donnés par le protocole AAPM, mais présentent une incertitude beaucoup plus faible de $\pm 0{,}2\%$. Si l'on utilise ces valeurs en suivant le protocole AAPM, il n'est plus nécessaire d'utiliser le facteur β_{cep}, puisqu'il est inclus dans ces valeurs calculées.

Zusammenfassung

Ansprechwahrscheinlichkeit von Ionisationskammern und Wand-Korrektionsfaktoren A_{Wand} für ^{60}Co-Strahlung mit Hilfe einer Monte-Carlo-Simulation.

Berechnet wurden Ansprechwahrscheinlichkeiten und Wand-Korrektionsfaktoren von Ionisationskammern für Großfeld-^{60}Co-Strahlung mit Hilfe von Monte-Carlo-Verfahren. Die berechneten Ansprechwahrscheinlichkeiten stimmen gut überein mit der Bragg-Gray-Hohlraumtheorie. Insbesondere fand man, daß die Ansprechwahrscheinlichkeit dividiert durch den Wand-Korrektionsfaktor A_{Wand} unabhängig ist von der Form des Detektors, aber abhängig vom Material der Kammerwand, so wie es von der Bragg-Gray-Theorie vorausgesagt wird. Eine einfache Theorie wird vorgestellt, mit deren Hilfe die Erhöhung der Ansprechwahrscheinlichkeit einer Farmer-Ionisationskammer, die durch eine Elektrode von beliebigem Material und Radius hervorgerufen wird, vorhergesagt werden kann. Die Änderungen der Ansprechwahrscheinlichkeit einer Kammer als Funktion der Zusammensetzung einer Verstärkerkappe stimmen gut überein mit analytischen Ausdrücken. Der Einfluß der Randeffekte in Flachkammern kann vernachlässigt werden. Bringt man während der Kalibrierung eine Flachkammer in ein flaches Phantom, so wird dadurch die Ansprechwahrscheinlichkeit erhöht um $1{.}0 \pm 0{.}2\%$. Die berechneten Werte von A_{Wand} stimmen gut überein mit den meisten experimentellen Ergebnissen, sowie mit den Ergebnissen der AAPM-Protokolle, jedoch mit einer beträchtlich geringeren Unsicherheit von $\pm 0{.}2\%$. Verwendet man diese Werte zusammen mit dem AAPM-Protokoll, so sollte der β_{cep}-Faktor nicht benutzt werden, da dieser in den berechneten Werten mit enthalten ist.

References

Attix F H 1979 *Health Phys.* **36** 347
——— 1984 *Med. Phys.* **11** 725–8
AAPM 1983 *Med. Phys.* **10** 741–71
Berger M J and Seltzer S M 1964 *Tables of Energy Losses and Ranges of Electrons and Positrons, Report NASA SP-3012* (Washington, DC: NASA)
——— 1983 *Stopping Powers and Ranges of Electrons and Positrons, Report NBSIR 82-2250-A* (Washington, DC: US Dept of Commerce)
Bielajew A F, Rogers D W O and Nahum A E 1985 *Phys. Med. Biol.* **30** 419–27

Boutillon M and Niatel M-T 1973 *Metrologia* **9** 139-46

Burlin T E 1968 in *Radiation Dosimetry* vol. 1 ed. F H Attix and W C Roesch (New York: Academic Press) p331

Henry W H 1980 private communication

Hubbell J H 1969 *Photon Cross Sections, Attention Coefficients and Energy Absorption Coefficients, Report NSRDS-NBS-29* (Washington, DC: NBS)

—— 1977 *Rad. Res.* **70** 58-81

ICRU 1984 *Radiation Dosimetry: Electron Beams with Energies between 1 and 50 MeV, Report 35* (Washington, DC: ICRU)

Johansson K A, Mattsson L O, Lindborg L and Svensson H 1978 *Int. Symp. on National and International Standardization of Radiation Dosimetry (Atlanta) 1977* (IAEA-SM-222/35) pp243-69

Kristensen M 1983 *Phys. Med. Biol.* **28** 1269-78

Loftus T P and Weaver J T 1974 *J. Res. Nat. Bur. Stand.* **78A** 465-76

McEwan A C and Smyth V G 1984 *Med. Phys.* **11** 216-8

NACP 1980 *Acta Radiol. Oncol. Radiat. Phys. Biol.* **19** 55-79

Nahum A E 1978 *Phys. Med. Biol.* **23** 24

Nahum A E, Henry W H and Ross C K 1985 *Phys. Med. Biol.* to be submitted

Nahum A E and Kristensen M 1982 *Med. Phys.* **9** 925-7

Nath R and Schulz R J 1981 *Med. Phys.* **8** 85-93

Niatel M T, Loftus T P and Oetzmann W 1975 *Metrologia* **11** 17-23

Rogers D W O 1984 *Nucl. Instrum. Methods Phys. Res.* **227** 535-48

Rogers D W O, Bielajew A F and Nahum A E 1983 *Med. Phys.* **10** 738 (abstract)

Schulz R J and Loevinger R 1984 *Med. Phys.* **11** 218

Spencer L V and Attix F H 1955 *Radiat. Res.* **3** 239-54